Earth's Future

RESEARCH ARTICLE
10.1029/2025EF006678

Climate-Driven Hydraulic Traits Shift in Natural and Planted Forests: Patterns, Drivers, and Future Acclimation

Yan Bai[1], Yujie Hu[1], Yanlan Liu[2], Kailiang Yu[3], Xiangzhong Luo[4], Liyao Yu[4], Lei Tian[5], and Jianping Huang[1]

[1]Collaborative Innovation Center for Western Ecological Safety, College of Atmospheric Sciences, Lanzhou University, Lanzhou, China, [2]School of Earth Sciences, The Ohio State University, Columbus, OH, USA, [3]Princeton Environmental Institute, Princeton University, Princeton, NJ, USA, [4]Department of Geography, National University of Singapore, Singapore, Singapore, [5]Key Laboratory of West China's Environmental System (Ministry of Education), Center for Dryland Water Resources Research and Watershed Science, College of Earth and Environmental Sciences, Lanzhou University, Lanzhou, China

Abstract Plants modify their functional traits in response to changing environmental conditions under climate change. However, it remains unclear whether tree planting alters patterns and acclimation of hydraulic traits across spatial scales. Here, we compiled a site-level data set of hydraulic traits in natural (NF) and planted forests (PF) to examine trait patterns and relationships, quantified environmental and ecological drivers on ecosystem-scale hydraulic traits of PF and NF across China, and computationally projected future trait acclimation using the space-for-time approach. We identified distinct differences in hydraulic traits between NF and PF, with PF exhibiting higher hydraulic safety but lower hydraulic efficiency than NF at the species level. NF demonstrated a trade-off between hydraulic efficiency and safety, whereas PF exhibited a contrasting positive correlation between these traits. We confirmed that both environmental and ecological factors influence ecosystem-scale hydraulic traits in NF and PF, although dominant drivers vary among specific traits. Projections under future climate scenarios suggest that, despite persistent differences in trait acclimation between NF and PF, both forest types tend to exhibit increased water-use efficiency and enhanced drought resistance in response to rising precipitation and air dryness. These findings provide a valuable benchmark for estimating potential changes in hydraulic traits under climate change, supporting improved simulations of carbon and water fluxes in response to climate and anthropogenic influences.

Plain Language Summary As the climate changes, plants adjust their characteristics to cope with new environmental conditions. However, it's not well understood whether tree planting affects how these adjustments happen across different areas. In this study, we compared the hydraulic traits (how trees move and store water) of trees in natural forests and planted forests across China. We found that planted forests have trees with better water safety but less efficient water use than trees in natural forests. Interestingly, in natural forests, there is a trade-off between water efficiency and safety, while in planted forests, these two traits seem to improve together. Both environmental factors (like weather) and ecological factors (such as tree age and height) affect these water traits, but the main influences vary. Looking ahead, we predict that both types of forests will become better at using water and resisting drought as a response to increasing rainfall and drier air. These findings are important for understanding how forests might change with climate change and for improving models that predict how forests impact the carbon and water cycles.

Key Points:

- Planted forests show higher hydraulic safety but lower efficiency than natural forests, with opposite trait trade-offs
- Environmental and ecological factors influence ecosystem hydraulic traits, but key drivers differ between natural and planted forests
- Both forest types tend to exhibit greater water-use efficiency and drought resistance despite differing acclimation patterns

Supporting Information:

Supporting Information may be found in the online version of this article.

Correspondence to:

Y. Bai and J. Huang,
yanbai@lzu.edu.cn;
hjp@lzu.edu.cn

Citation:

Bai, Y., Hu, Y., Liu, Y., Yu, K., Luo, X., Yu, L., et al. (2026). Climate-Driven Hydraulic Traits Shift in Natural and Planted Forests: Patterns, Drivers, and Future Acclimation. *Earth's Future*, *14*, e2025EF006678. https://doi.org/10.1029/2025EF006678

Received 10 JUL 2025
Accepted 22 DEC 2025

Author Contributions:

Conceptualization: Yan Bai, Yanlan Liu
Data curation: Yan Bai, Yujie Hu, Kailiang Yu, Xiangzhong Luo, Liyao Yu
Formal analysis: Yan Bai, Yujie Hu, Yanlan Liu, Kailiang Yu, Xiangzhong Luo, Liyao Yu, Lei Tian
Funding acquisition: Yan Bai, Jianping Huang
Investigation: Yan Bai, Yujie Hu
Methodology: Yan Bai, Yanlan Liu
Project administration: Yan Bai, Jianping Huang
Resources: Yan Bai, Yujie Hu, Yanlan Liu, Kailiang Yu, Jianping Huang
Software: Yan Bai
Supervision: Yan Bai, Yanlan Liu, Jianping Huang

1. Introduction

Understanding how terrestrial plants respond physiologically to environmental stresses is crucial for predicting land-surface water, carbon and energy exchanges under future climate change (McDowell et al., 2019). Water transports vertically from the soil to plant roots, stems, and leaves along with a water potential gradient, eventually transpiring through leaf stomata into the atmosphere (Sperry & Love, 2015). This process, known as plant hydraulics, is considered a crucial link connecting soil and atmospheric water stress to leaf gas exchange (Wang et al., 2019; Wang & Frankenberg, 2024) and represents an internally consistent evolutionary optimization, through which plants have co-evolved hydraulic and stomatal traits to maximize long-term carbon gain (Anderegg & Venturas, 2020). Plant hydraulics processes regulated by hydraulic traits can be influenced by changing environmental conditions due to both climate change and human activities such as afforestation-led

Validation: Yan Bai
Visualization: Yan Bai, Yujie Hu, Kailiang Yu
Writing – original draft: Yan Bai, Xiangzhong Luo, Liyao Yu, Lei Tian
Writing – review & editing: Yan Bai

changes in land use (Liu et al., 2020). However, critical traits related to hydraulic efficiency (i.e., the maximum sapwood-specific hydraulic conductivity, K_s) and safety (i.e., the xylem water potential at which 50% of hydraulic conductivity is lost, $P50_x$) and their trade-off may differ significantly between those in natural (NF) and artificially planted forests (PF), indicating their divergent water storage and transport processes (Hua et al., 2022; Shangguan et al., 2022; Ye, 2021; Yi et al., 2021). These key hydraulic traits play important roles in future ecosystem-atmosphere feedback effects in a changing climate (Anderegg et al., 2018). Therefore, detecting the regulation of plant hydraulics under the impact of tree planting and implementing it into land surface and climate models will be beneficial to improve simulations of carbon and water fluxes under future climate change and anthropogenic influences.

Tree planting has been proposed as a potentially effective solution for mitigating climate change (Louman et al., 2019). Since the 1970s, China has implemented the world's largest afforestation and reforestation project (Yu et al., 2018). China's planted forest (PF) covered a total area of 7.70×10^5 km^2 till 2020, accounting for 31.30% of the world's total PF (Cheng et al., 2023). Recently, the China Plant Trait Database (Wang, Harrison, et al., 2022) and the Global Ecosystem-scale Hydraulic Trait Data set (Liu, Holtzman, & Konings, 2021) have been released, which would be helpful to investigate plant hydraulics dynamics for PF. However, these data sets lack the classification of tree trait data by natural and planted environmental conditions. Some studies conducted at Chinese sites have found that natural forest (NF) often exhibits higher xylem hydraulic efficiency, but weaker cavitation resistance compared to PF within the same species (Shangguan et al., 2022; Ye, 2021). Although theoretical research suggests a trade-off between xylem hydraulic efficiency and safety (Jin et al., 2024; Sperry, 2003), only a weak trade-off in evergreen angiosperms in NF, but not in PF, has been demonstrated in China (Ye, 2021). Therefore, there is an imperative requirement to compile a comprehensive data set to facilitate an in-depth analysis of the overall picture of key hydraulic traits in NF and PF species, and uncover the physiological mechanisms of plant hydraulics under the impact of climate change and human activities.

The functional traits of tree species can be modulated by the environment via acclimation, and the coordination of these traits has also been shown to be strongly linked with climate (Reich, 2014). With the global consequences of climate change, for example, rising atmospheric vapor pressure deficit (VPD) and more frequent drought events (Grossiord et al., 2020), many tree species tend to modify their functional traits and optimize their fitness in response to changing environmental conditions (Liu, Ye, et al., 2022). This regulation, known as trait acclimation, is a crucial mechanism by which plants acclimate and survive under climate change (Nicotra et al., 2010). It has been demonstrated that the diversity in hydraulic and photosynthetic traits is more closely related to the local water availability than overall species diversity (Trugman et al., 2020). It has also been reported that environmental conditions, rather than evolutionary history, are the primary factors of variation in the acclimation of plant hydraulic traits (Liu, Ye, et al., 2022). Therefore, it is possible to predict the acclimation of tree hydraulic traits in response to changing environmental conditions. Meanwhile, human activities, such as afforestation, potentially change the individuals in forests which have different hydraulic traits than endemic species, and can also artificially change environments to further induce changes in traits (Liao et al., 2012). These disparities between natural and planted species lead us to propose that hydraulic traits adjust to temporal changes in climate to the same degree as they adapt to climate variations across spaces (Liu, Ye, et al., 2022). This theory offers a valuable tool for utilizing the current correlations between NF and PF species' traits and environmental factors to forecast their future traits under climate change.

Here, assuming that there exist differences in the patterns and acclimation of hydraulic traits of NF and PF species under climate change, this study aims to (a) quantify differences in hydraulic traits (i.e., K_s, $P50_x$) and their trade-off in NF and PF using a data set of site-level tree hydraulic traits in China, (b) assess controls of ecosystem-scale hydraulic traits in NF and PF by quantifying the dependence of hydraulic traits on environmental and ecological drivers, and (c) identify the acclimation capacity of hydraulic traits in NF and PF by examining future trends of hydraulic traits under climate change. Our study aims to provide a baseline to assess current patterns and future acclimation of tree hydraulic traits in China, which will improve our understanding of physiological mechanisms of plant hydraulics, and improve simulations of carbon and water fluxes under future climate change and anthropogenic influences.

2. Materials and Methods

2.1. Data Compilation

2.1.1. Site-Level Key Hydraulic Traits in China

We compiled a site-level data set of plant hydraulic traits, including xylem hydraulic efficiency K_s and safety $P50_x$ in NF, PF, and shrubs, and categorized the data into two groups, that is, cross-species comparison (CSC) sites and within-species comparison (WSC) sites. The CSC data set was primarily derived from a meta-analysis, including 10 publications (covering 20 sites and 225 species) from Liu et al. (2019, 2021a), which were classified into NF and PF based on site descriptions in the original studies. Additionally, we integrated data from 23 Chinese and English publications collected over the past two decades across China (covering 29 sites and 112 species), resulting in a CSC data set comprising 33 publications, 49 sites, and 309 woody plant species. The WSC data set combined results from meta-analyses and our own field measurements. Two publications (Shangguan et al., 2022; Ye, 2021) provided paired NF and PF data for the same species in humid regions of southern China (3 sites, 14 species), while our field observations in drylands of northern China contributed additional data (2 sites, 1 species), yielding a WSC data set that includes 3 publications, 5 sites, and 15 species. Together, these data sets provide a robust foundation for evaluating cross-species and within-species differences in hydraulic traits between NF and PF. Detailed experimental protocols for traits we observed can be found in Text S1 of Supporting Information S1, and the site-level trait data set and its Supporting Information S1 are provided in Table S1 and Text S2 of Supporting Information S1.

2.1.2. Ecosystem-Scale Hydraulic Traits in China

The site-level data set of tree hydraulic traits in NF and PF was obtained through ground-based measurements and provides detailed physiological insights into hydraulic traits of NF and PF. However, due to its limited spatial coverage, it is challenging to investigate patterns and acclimation of hydraulic traits of NF and PF over a larger spatial scale. To address this limitation, we extracted ecosystem-scale hydraulic traits in China from the Global Ecosystem-scale Plant Hydraulic Traits, which were retrieved from a plant hydraulic model using model-data fusion (Liu, Holtzman, & Konings, 2021). Hydraulic traits were estimated as distributions, with the spread representing trait uncertainty. These ecosystem-scale hydraulic traits include: vegetation capacitance parameter related to plant water potential (C), the sensitivity parameter of stomatal conductance to vapor pressure deficit VPD (g_1), maximum xylem conductance ($g_{p,max}$), leaf water potential when maximum carboxylation rate drops to half of its maximum value under well-watered conditions ($P50_s$) and $P50_x$ (Table S2 in Supporting Information S1). To distinguish ecosystem-scale hydraulic traits of NF and PF pixels, we used a map depicting the distribution of NF and PF in China from the China Vegetation Products data set (Cheng et al., 2023; Figure 1), and unified its spatial resolution with ecosystem-scale hydraulic traits at 0.25° resolution. We then extracted traits of NF and PF based on their spatial distribution, which finally resulted in a data set of ecosystem-scale hydraulic traits of NF and PF in China. The observation period for the remote sensing data set used to retrieve the traits, as well as the forest inventory period for the China Vegetation Products data set, was both between 2004 and 2005, retrieved traits therefore represent the NF and PF traits. Liu, Holtzman, and Konings (2021) reported discrepancy between the site-level and the ecosystem-scale $P50_x$ due to species diversity, canopy structure, and demographic composition. We also compared the aggregated site-level $P50_x$ and the ecosystem-scale $P50_x$, and found similar discrepancy of $P50_x$ of NF, PF and SH species between the site and ecosystem scale (Figure S1 in Supporting Information S1).

2.1.3. Ecosystem-Scale Environmental and Ecological Factors

To further investigate environmental and ecological controls on ecosystem-scale hydraulic traits in China, we collected 10 environmental (ENV) and 5 ecological factors (ECO) potentially related to hydraulic traits at 0.25° resolution. All of factors were derived from observations in the growing season of 2004 and 2005, which were consistent with the retrieval time of ecosystem-scale hydraulic traits from Liu, Holtzman, and Konings (2021). ENV factors include air temperature (T_a), soil temperature (T_s), precipitation (P_r), surface air pressure (P_s), and net shortwave radiation (R_n) derived from the Global Land Data Assimilation System (GLDAS) (Beaudoing et al., 2020; Rodell et al., 2004), VPD calculated by T_a, P_s and specific humidity (Q) (Campbell & Norman, 1998), aerodynamic conductance (G_a) calculated by the ratio between the sensible heat net flux and the difference between air and surface skin temperatures (Liu, Holtzman, & Konings, 2021), shallow soil moisture (M_s)

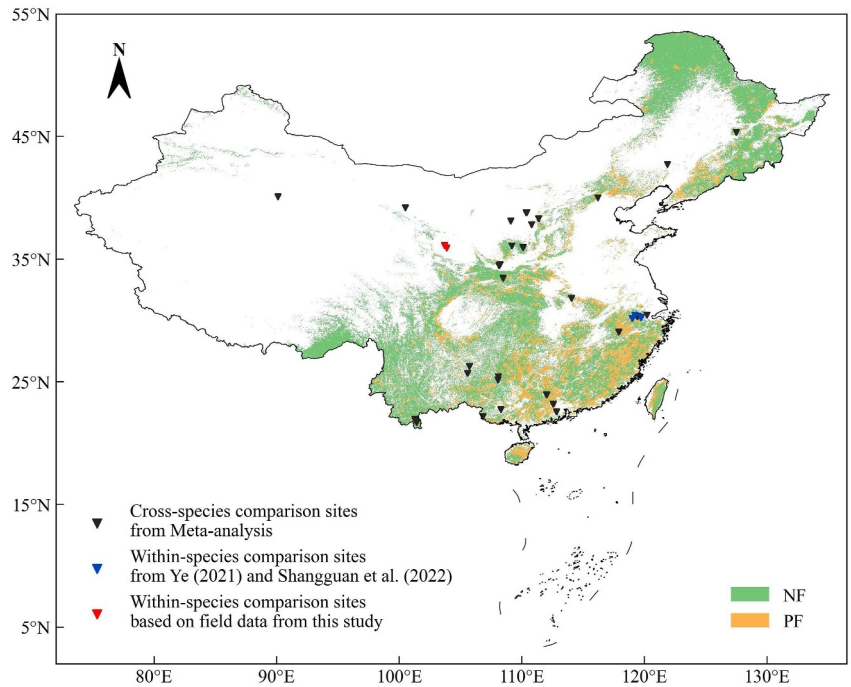

Figure 1. The map depicting the distribution of natural (NF) and planted forests (PF) based on Cheng et al. (2023) and study sites of hydraulic traits in China.

extracted from Advanced Microwave Scanning Radiometer for EOS (AMSRE) data set (Parinussa et al., 2016), potential evapotranspiration (PET) calculated by the Penman-Monteith equations (Allen et al., 1998), and dryness index (DI) calculated by the ratio of PET and P_r. ECO factors include Leaf area index (LAI) derived from Moderate Resolution Imaging Spectroradiometer (MODIS) data set MCD15A3H (Myneni et al., 2015), vegetation optical depth (VOD) extracted from the AMSRE data set, canopy height (H_c) extracted from the global map of forest height (Liu, Su, et al., 2022), forest age (A_t) derived from the China's annual forest age data set (Cheng et al., 2024), and maximum rooting depth (R_d) obtained from a global synthesis of observations (Fan et al., 2017). Detailed information about ecosystem-scale ENV and ECO factors is available in Table S2 of Supporting Information S1.

2.2. Data Analysis

2.2.1. Comparisons of Site-Level Hydraulic Traits and Their Relations in NF and PF

We conducted data analyses for NF and PF species in China separately, compared their hydraulic efficiency K_s and safety $P50_x$, as well as their hydraulic efficiency–safety relations across sites. Based on the specific data set as described in Section 2.1.1., we also tested whether differences in hydraulic traits and their relations in NF and PF exist at WSC sites (Figure S2 in Supporting Information S1). The original values of $P50_x$ and $P50_s$ were negative. We used their absolute values to represent hydraulic safety, where a larger absolute value indicates stronger hydraulic safety, and thus, the unit is expressed as -MPa. For the analysis of the trade-off between xylem hydraulic efficiency and safety, we performed a logarithmic transformation on $P50_x$ to homogenize its variance. Additionally, previous studies have demonstrated a clear and strong trade-off between hydraulic efficiency K_s and safety $P50_x$ in shrub (SH) species (Huo et al., 2022; Yao et al., 2021), we thus provided hydraulic traits and their relations of SH species as a reference to NF and PF species.

2.2.2. Determine Drivers of Ecosystem-Scale Hydraulic Traits in NF and PF

To understand environmental and ecological controls of hydraulic traits at a larger scale, we examined correlations among ecosystem-scale hydraulic traits, ENV and ECO factors in NF and PF pixels, and the correlation of each trait to ENV and ECO factors was calculated as the Pearson's R of the relationship between each trait and

ENV and ECO factors, respectively (Figure S3 in Supporting Information S1). We further developed a weight least squared (WLS) regression model to explain each of ecosystem-scale hydraulic traits (i.e., C, g_1, $g_{p,max}$, $P50_s$, $P50_x$) using ENV and ECO factors, respectively (Strutz, 2016):

$$y_i = \sum_{j=1}^{j=m} a_{ij}\, x_{env,ij} + \sum_{k=1}^{k=n} b_{ik}\, x_{eco,ik} + c_i \quad (1)$$

where y_i is the ith trait; $x_{env,ij}$ is the ENV driver j for the ith trait; $x_{eco,ik}$ is the ECO driver k for the ith trait; c_i is the intercept; a_j and b_k are the regression coefficients of ENV and ECO factors, respectively, which were optimized by minimizing the following error function S:

$$S = \sum_{i=1}^{n} W_i \left(\widehat{y_i} - y_i\right)^2 \;\rightarrow\; \min, (i = 1, 2, \ldots, n) \quad (2)$$

where $\widehat{y_i}$ is the modeled value of the ith trait, and the weight W_i is calculated by the reciprocal of the difference between the 95th percentile and 5th percentile of the retrieved ith trait. The weights were utilized to quantify the representativeness of the posterior mean traits (y_i) obtained through Bayesian inference, which vary across space due to the effectiveness of observational constraints employed to retrieve the traits (Liu, Holtzman, & Konings, 2021). A broader posterior distribution (with a larger difference between the 95th percentile and 5th percentile) indicates a lower precision of the retrieved trait, and thus should be considered with a lower weight in estimating trait-environment relationships.

To reduce the uncertainty in simulation results caused by collinearity among driving factors, we monitored the variance inflation factor (VIF) of all 15 driving factors. For highly correlated variables (such as temperature and VPD, and between different precipitation indices), we retained only the one most directly related to plant hydraulics, ensuring that the VIF value of selected variables was below the commonly used threshold of 10. This process resulted in the final model driver data set, where ENV factors included R_n, VPD, P_r, P_s, M_s, and G_a, and ECO factors included D_r, LAI, VOD, A_t, and H_c (Figure S4 in Supporting Information S1). To further identify the most informative drivers of each trait, we conducted model selection, ensuring at least one variable was chosen from each category (i.e., ENV and ECO). The performance of models with different driver combinations was evaluated using the coefficient of determination (R^2) and the Akaike information criteria (AIC). For each trait, we selected the model with the least AIC and the highest R^2 as the best-performance model. All factors were normalized by z-score prior to conducting the WLS analyses. Factor sensitivities were then calculated based on the regression coefficient from the WLS simulation.

2.2.3. Identify the Acclimation of Ecosystem-Scale Hydraulic Traits in NF and PF

Based on the assumption of trait acclimation, that is, hydraulic traits adjust to temporal changes in climate to the same degree as they adapt to climate variations across spaces, we predicted future trends of ecosystem-scale hydraulic traits under climate change. We introduced future ENV factors into the best-fitting models of NF and PF using the Phase 6 of the Coupled Model Intercomparison Project (CMIP6) data set. We selected MRI-AGCM3-2-H and MRI-AGCM3-2-S models (Mizuta et al., 2019a, 2019b) from CMIP6 for the following reasons: (a) monthly ENV factors are available in both historical and future simulations; (b) their high spatial resolution (25 km) is necessary to differentiate between NF and PF pixels; (c) their long-term range (2000–2100) aligns with the time scale of acclimation. To evaluate the long-term climate conditions in NF and PF pixels, we used four ENV factors (i.e., R_n, P_s, P_r and VPD) from the two CMIP6 models. We further calculated annual mean values of ENV factors in these two CMIP6 models based on their monthly data, and introduced them into the best-fitting models.

Both GLDAS observations and CMIP6 simulations exhibit biases. To mitigate the impact of systematic bias while retaining the dynamics of the four ENV factors, we employed a commonly used cdf-matching (cumulative distribution function) method (Kamruzzaman et al., 2019; Liu, Holtzman, & Konings, 2021), which avoids direct comparison between GLDAS-derived and CMIP6-predicted ENV factors:

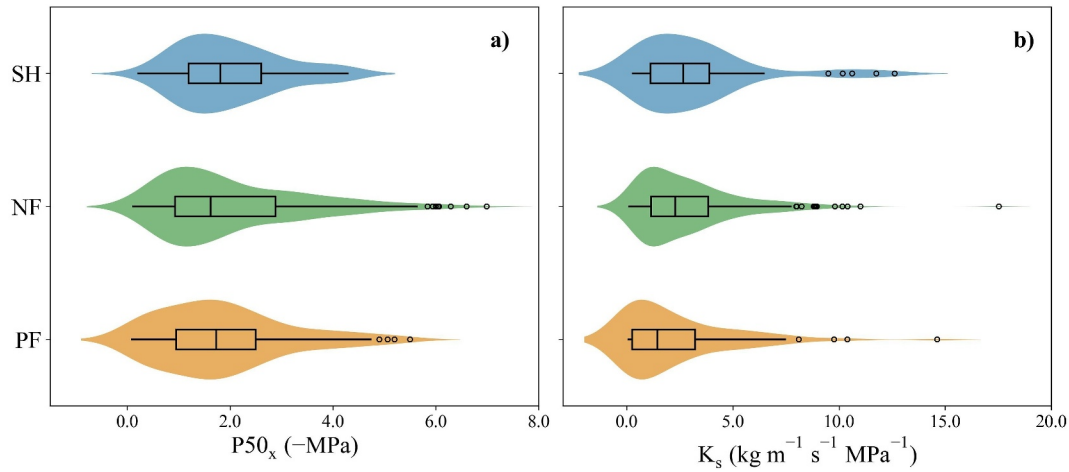

Figure 2. Hydraulic safety $P50_x$ (a) and hydraulic efficiency K_s (b) among shrubs (SH), natural forests (NF) and planted forests (PF) across China.

$$x'_p(t) = x_p(t) + F^{-1}_{\text{obs}}\{F_{p.\text{sim}}[x_p(t)]\} - F^{-1}_{r.\text{sim}}\{F_{p.\text{sim}}[x_p(t)]\} \quad (3)$$

where $x'_p(t)$ and $x_p(t)$ are the bias-corrected data and the raw data of future projections on the month t, respectively; $F(\theta)$ and $F^{-1}(\theta)$ denote the cdf of the monthly data θ and its inverse, respectively; the subscripts p.sim, r.sim, and obs are the future projection (2024–2100), retrospective simulation in the averaged CMIP6 model (2000–2024), and the observed GLDAS data (2000–2024), respectively. This cdf-matching calibration harmonized the variability between the CMIP6 and GLDAS data while preserving the predictive trends of ENV factors in CMIP6 (Figure S5 in Supporting Information S1).

Based on the best-fitting models and future cdf-modified ENV factors, we predicted future trends of hydraulic traits in NF and PF across China from 2024 to 2100 under the impact of acclimation. To quantify the uncertainty in future trait trends, we employed a bootstrapping approach with the following steps: (a) a combination of regression coefficients was randomly generated from the multivariate Gaussian distribution in the prediction model; (b) likewise, the trait was predicted according to the prediction model with the generated regression coefficients; (c) the linear trend of the trait was then estimated and plotted. This procedure was repeated for 200 times for each of the five traits in NF and PF, resulting in 200 estimated trends of each trait in NF and PF under future climate. Additionally, to convert the high-resolution 1 km forest spatial distribution map into the 0.25° resolution required by the WLS model, we employed a majority-rule approach to assign each 0.25° pixel the forest type (i.e., blank, NF, or PF) with the highest proportion within that pixel. We further applied varying minimum proportion thresholds to filter the classification results (Figure S6 in Supporting Information S1), thereby generating 0.25° resolution maps of NF and PF. Based on these maps, we reclassified ENV and ECO driver data sets for NF and PF, and reran the WLS models to assess the uncertainty in hydraulic trait predictions induced by the change in forest distribution resolution (Figure S7 in Supporting Information S1). Given that a 50% threshold yielded insufficient PF coverage and that predictions within the 35%–45% threshold range showed relatively low uncertainty (Figure S6 in Supporting Information S1), we adopted the 40% threshold-based forest distribution to derive the final estimates of trait acclimation.

3. Results

3.1. Patterns of Site-Level Hydraulic Traits and Their Relations in NF and PF

To determine whether there exist differences in current acclimation capacity of NF and PF species, we conducted a comparison of site-level hydraulic traits of NF and PF, as well as SH in the entire data set (Figure 2). Results showed that, SH exhibited a more concentrated distribution of $P50_x$, followed by PF and NF, while NF had lower median $P50_x$ (1.62 -MPa) than that of PF (1.73 -MPa) (Figure 2b). The results indicated that the hydraulic safety of NF was comparatively lower and more variable than that of PF, although the overall difference between the two

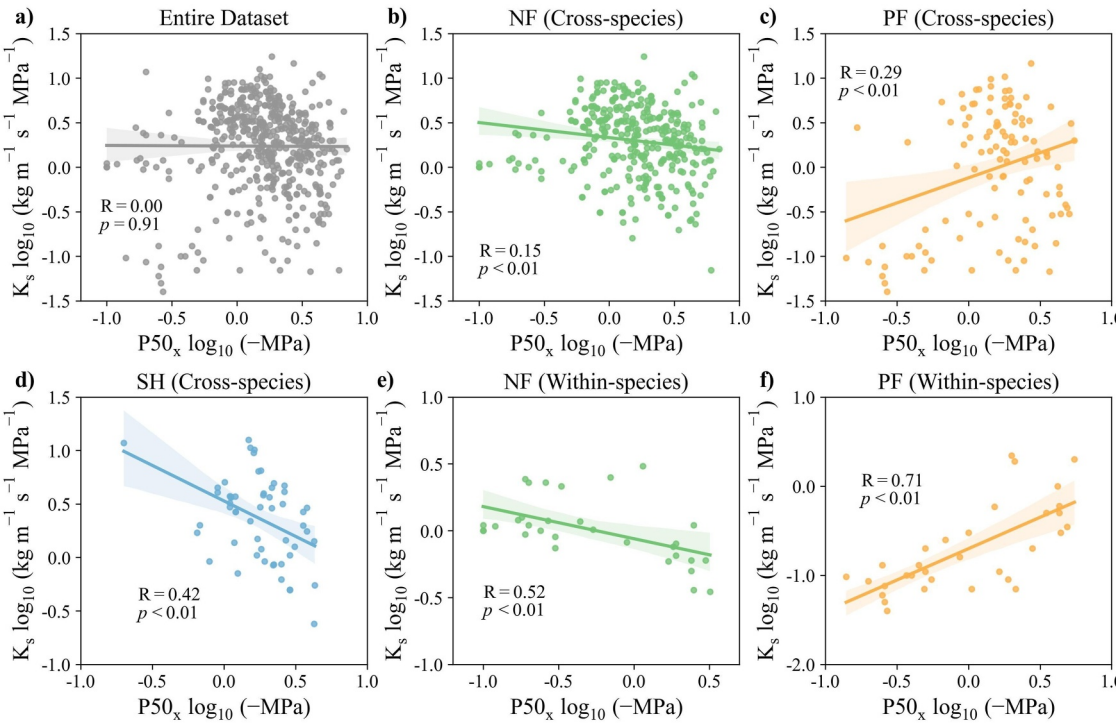

Figure 3. Relationship between hydraulic efficiency (K_s) and safety ($P50_x$) in the entire data set (a), in natural forest (NF) at cross-species comparison sites (b), in planted forest (PF) at within-species comparison sites (c), in shrubs (SH) at cross-species comparison sites (d), in NF at within-species comparison sites (e), and in PF at within-species comparison sites (f). Data plotted on log-transformed axes.

is not significant ($p = 0.24$). Meanwhile, the median K_s of SH was the highest (2.67 kg m^{-1} s^{-1} MPa^{-1}), followed by NF (2.29 kg m^{-1} s^{-1} MPa^{-1}), and PF was the lowest (1.45 kg m^{-1} s^{-1} MPa^{-1}) (Figure 2b). These results indicated that SH exhibited the highest hydraulic efficiency, followed by NF and PF, with a significant difference observed between NF and PF across sites ($p < 0.05$). Notably, we also investigated trait differences of NF, and PF at WSC sites (Figure S2 in Supporting Information S1). It was found that when comparing with same species, most NF species (12 out of 15) had lower $P50_x$ (1.03 ± 1.03 -MPa), but higher K_s (1.19 ± 0.71 kg m^{-1} s^{-1} MPa^{-1}) than that PF species (1.68 ± 1.66 -MPa, 0.39 ± 0.58 kg m^{-1} s^{-1} MPa^{-1}, respectively). These results further demonstrate that there are differences in hydraulic traits between the same species of NF and PF, with the difference in hydraulic efficiency being more significant than hydraulic safety.

Theoretical research suggests a trade-off between xylem hydraulic efficiency and safety (Sperry, 2003). As such, we conducted tests to investigate the existence of this trade-off among SH, NF, and PF species (Figure 3). Our research confirmed that there was no significant trade-off between K_s and $P50_x$ in the entire data set ($R = 0.00$, $p = 0.91$). However, the most significant trade-off existed in the SH species ($R = 0.42$, $p < 0.01$; Figure 3d). This negative relationship appeared in the NF species ($R = 0.15$, $p < 0.01$; Figure 3b), but a positive relation was found in PF species ($R = 0.29$, $p < 0.01$; Figure 3c) at CSC sites. Further investigation at WSC sites showed that, there was a strong trade-off hydraulic efficiency–safety for NF species ($R = 0.52$, $p < 0.01$; Figure 3e), but still a significant positive relation for PF species ($R = 0.71$, $p < 0.01$; Figure 3f). These findings demonstrate that in natural species (i.e., SH and NF), there is a significant hydraulic efficiency–safety trade-off. However, it is possible that hydraulic safety and efficiency compensate for each other to facilitate photosynthesis, which may lead to a positive correlation between hydraulic efficiency and safety in planted forests.

3.2. Drivers of Ecosystem-Scale Hydraulic Traits in NF and PF

To investigate how environmental and ecological factors influence tree hydraulic traits at a larger scale, we assessed correlations between ecosystem-scale hydraulic traits and their driving factors. We found that hydraulic traits in both NF and PF exhibited notable correlations with both ENV and ECO factors, with particularly strong associations observed for the traits g_1 and $g_{p,max}$ across nearly all factors (Figure S3 in Supporting

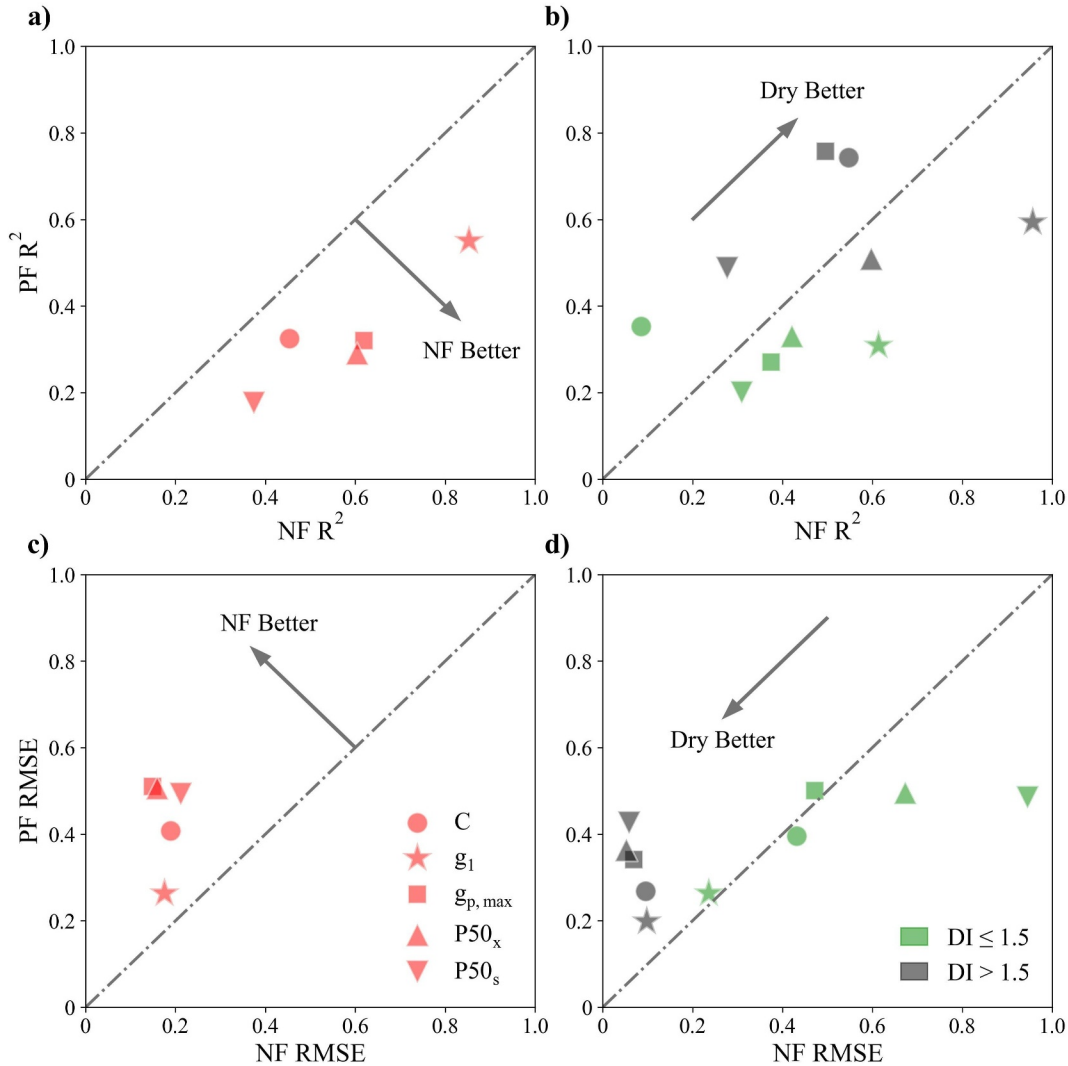

Figure 4. Model performance in estimating ecosystem-scale hydraulic traits. The performance of planted forests (PF) and natural forests (NF) was evaluated using the coefficient of determination R^2 (a, b) and the standardized root mean square error RMSE (c, d) for each trait (a, c) and across different climatic regions (b, d), which were categorized as humid regions (dryness index, DI ≤ 1.5) and drylands (DI > 1.5).

Information S1). Based on the WLS simulation, we identified the most informative drivers within each group of ENV and ECO using AIC. We evaluated the performance of the NF and PF models using R^2 and the standardized RMSE for each trait and across regions classified as humid regions (DI ≤ 1.5) and drylands (DI > 1.5), as defined by Huang et al. (2016). As illustrated in Figure 4, all traits of the NF models exhibited higher R^2 (Figure 4a) and lower RMSE (Figure 4c) than those of the PF models, indicating that NF traits were more tightly controlled by ENV and ECO factors. When diagnosing the connection of ENV and ECO factors to traits in humid regions and drylands separately, it was noteworthy that traits in drylands were more closely coupled with ENV and ECO factors, as evidenced by higher R^2 values and lower RMSE scores (Figures 4b and 4d). This finding suggests that ENV and ECO factors play a more significant role in shaping traits in drylands compared to humid regions.

The factor sensitivity analysis further confirmed that both ENV and ECO factors influence hydraulic traits in NF and PF, but the dominant drivers vary across traits (Figure 5). For instance, the sensitivity of C to most factors was significantly lower in NF compared to PF. In NF, g_1 exhibited the strongest negative sensitivity to R_n and the highest positive sensitivity to A_t, whereas in PF, g_1 was most negatively sensitive to VOD and most positively sensitive to P_r. The variation in $g_{p,max}$ was primarily driven by VPD in NF, but by P_r in PF. In terms of P50, NF showed the greatest sensitivity to D_r and H_c, while in PF, xylem $P50_x$ was sensitive to multiple ENV and ECO

10.1029/2025EF006678

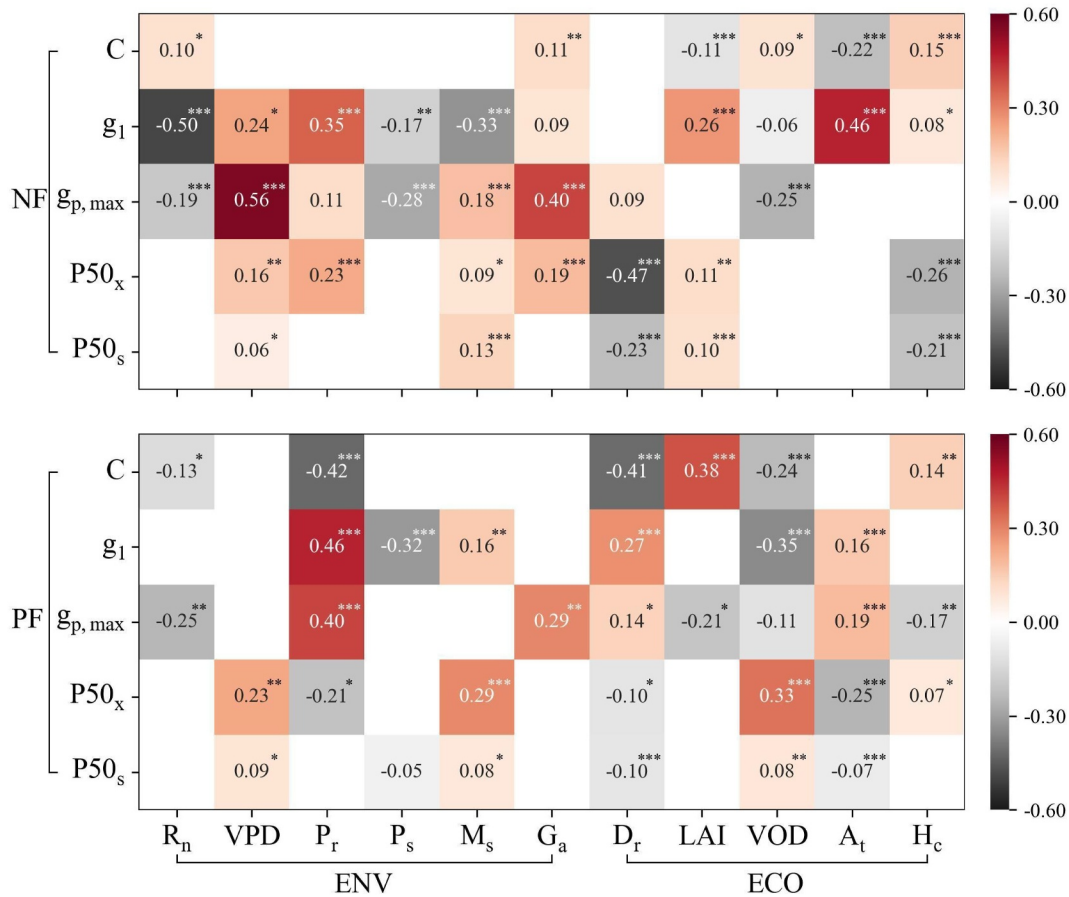

Figure 5. Factor sensitivity in estimating ecosystem-scale hydraulic traits of planted forests (PF) and natural forests (NF) using weighted least square regressions. Driving factors were grouped into two categories: environmental (ENV) and ecological factors (ECO). Blank means that the factor was excluded during the selection process based on the Akaike Information Criterion.

factors, whereas leaf $P50_s$ exhibited minimal sensitivity to most predictors. These results highlight that the combined effects of ENV and ECO variables shape the current patterns of hydraulic traits in both NF and PF. In addition, the standard deviations of sensitivity estimates indicated that PF exhibited greater uncertainty in factor sensitivity than NF (Figure S8 in Supporting Information S1), implying higher uncertainty in the future acclimation of PF traits.

3.3. Prediction of Trait Acclimation of NF and PF Under Future Climate

To assess potential changes in hydraulic traits of NF and PF under climate change, we applied the best-fitting models that explicitly link trait variation to climatic drivers, and predicted future trends and uncertainties of ecosystem-scale hydraulic traits based on the assumption of acclimation. The results indicated that under future climate change, the water storage parameter C of NF is projected to increase slightly, whereas C in PF tends to decline (Figure 6a), though this trend is accompanied by high uncertainty, as reflected by the wider spread of the shaded lines. Both NF and PF show an upward trend in g_1, yet with considerable uncertainty (Figure 6b), largely attributed to the high sensitivity of g_1 to P_r (Figure 5), whose future trajectory is highly variable (Figure S5 in Supporting Information S1). The $g_{p,max}$ of NF shows a significant increase, while PF exhibits a weaker and statistically non-significant trend ($p = 0.36$, Figure 6c), again due to the strong influence of P_r, the most sensitive driver for this trait. Both leaf and xylem P50 values in NF and PF show significant upward trends in response to rising VPD (Figure 5 and Figure S5 in Supporting Information S1), indicating enhanced drought resistance. Notably, the projected $P50_s$ of NF and PF tend to converge in the future, while differences in $P50_x$ between NF

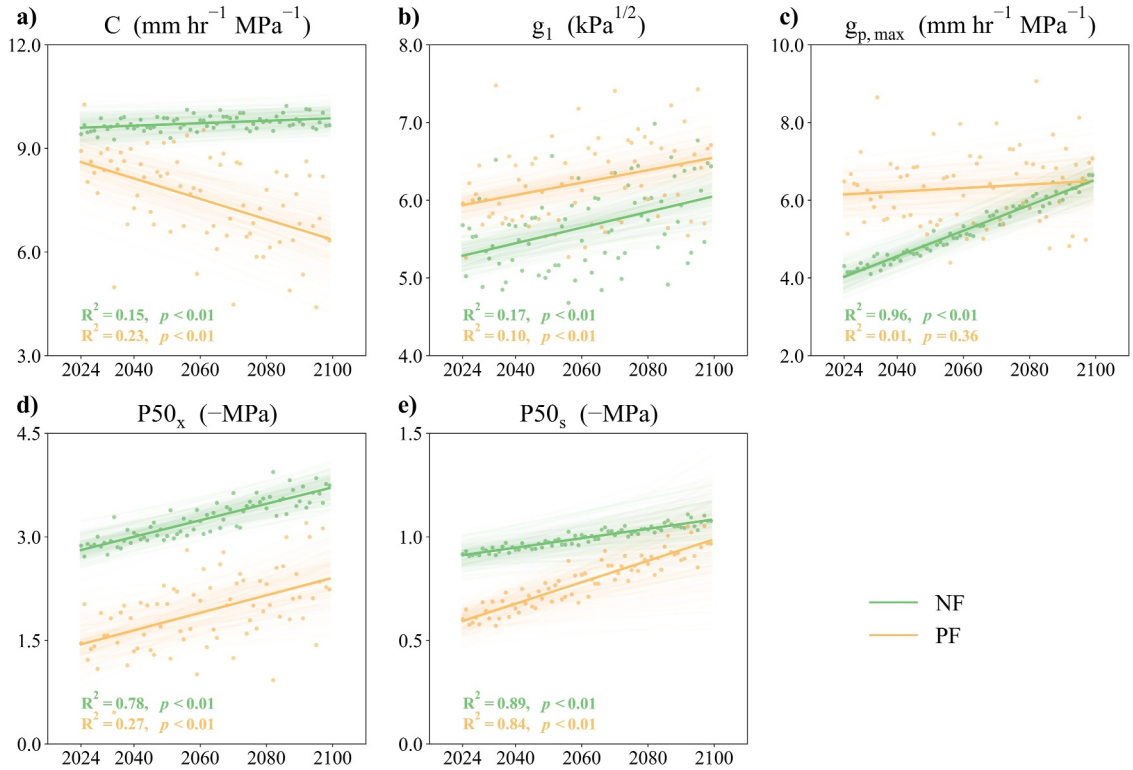

Figure 6. Future trends of natural forests (NF) and planted forests (PF) from 2024 to 2100 under the impact of acclimation. The green and yellow lines represent trends of NF and PF traits. The light lines are regression lines from the bootstrapping strategy.

and PF are expected to persist. Overall, despite shared tendencies toward improved hydraulic function, the differences in climate-driven trait acclimation between NF and PF are likely to remain over the long term.

4. Discussion

4.1. Different Patterns of Site-Level Hydraulic Traits in NF and PF

We confirmed differences in hydraulic efficiency and safety between NF and PF both cross-species and within-species (Figure 3). Cross-species comparisons revealed that NF generally exhibited lower hydraulic safety (albeit not significantly) and higher hydraulic efficiency than PF (Figure 2). Notably, when comparisons were conducted within the same species, the pattern of higher hydraulic safety and lower hydraulic efficiency in PF became more pronounced, with 12 out of 15 PF species in the WSC data set supporting this trend (Figure S2 in Supporting Information S1). Hydraulic traits were collected for the same species with similar tree diameters, heights, ages, and canopy widths in these sites, thereby eliminating the impact of ecological factors on the observation of traits (Shangguan et al., 2022; Ye, 2021). Previous studies reported that deciduous angiosperms in natural habitats improve water transport efficiency to mitigate the effects of decreased soil water availability and increased transpiration demand, thus reducing their reliance on embolism resistance (Hajek et al., 2016; Maherali et al., 2004). The main environmental difference between the manipulated and natural habitats was the higher soil water availability in the former, which was achieved through artificial irrigation (Shangguan et al., 2022; Ye, 2021). This may explain why the hydraulic traits of PF differ from those of NF. Regarding the trade-off between hydraulic efficiency and safety, we found that shrubs exhibit a significant tradeoff (Figure 4d), which is in line with recent research on shrubs (Huo et al., 2022; Yao et al., 2021). Previous studies reported that the hydraulic efficiency-safety trade-off is not significant across species (Liu, Ye, et al., 2022), which is also consistent with our study (Figures 3b and 4c).

Contrary to the trade-off between hydraulic efficiency and safety observed in NF (Figures 3b and 3e), PF showed an increase in hydraulic efficiency with enhanced safety at both cross-species and within-species sites (Figures 3c and 4f). Previous studies have demonstrated that greater hydraulic safety is beneficial for improving the amount

of water extracted by plants, thereby avoiding hydraulic failure during severe water stress (Lu et al., 2020). Wang, Ding, et al. (2022) reported that increased hydraulic safety compensates for hydraulic efficiency, thereby maintaining photosynthesis. This compensation effect in xylem functions is the dominant force facilitating photosynthetic rates from species to phylum scale. In this study, the compensation effect was particularly pronounced in PF, possibly due to improved water transport efficiency and high carbon sequestration capacity with sufficient water availability in these cultivated ecosystems. However, further research with larger sample sizes would be needed to test this hypothesis in a more rigorous manner.

4.2. Contrasting Drivers of Ecosystem-Scale Hydraulic Traits in NF and PF

While the vast majority of research focuses on inter- and intra-species differences in tree hydraulic traits, relationships between these traits and environmental and ecological forcings are less understood, and are crucial for modeling the impact of climate on vegetation (Anderegg, 2015). Previous studies reported that hydraulic traits are related to climatic seasonality (Liu, Ye, et al., 2021), and they are coordinated with plant height across aridity gradients (Liu et al., 2019), indicating that both environmental and ecological factors contribute to spatial and temporal variation in plant hydraulic traits. However, a community-weighted average of hydraulic traits may not accurately represent the integrated hydraulic behavior at an ecosystem scale (Anderegg et al., 2018; Liu, Holtzman, & Konings, 2021). Our WLS analyses confirmed that hydraulic traits in both NF and PF are simultaneously influenced by ENV and ECO factors, though dominant drivers vary among traits (Figure 5). Given the joint influence of ENV and ECO drivers on current NF and PF hydraulic traits, assuming that spatial trait-climate relationships can serve as a proxy for temporal trait changes, the observed differences in factor sensitivity between NF and PF imply divergent future climate acclimation trajectories for NF and PF (Figure 6). Furthermore, hydraulic traits in drylands were much closely related to their driving factors (Figure 4b), likely reflecting tighter physiological coupling of hydraulic function with water availability (Rosas et al., 2019). This finding is consistent with our site-level results, which show that differences in water availability between NF and PF habitats contributed to the observed divergence in hydraulic traits.

Note that ecosystem-scale hydraulic traits assessed in this study represent effective traits representing ecosystem-scale property. A single pixel may contain a mixture of forest types, potentially leading to blurred boundaries between NF and PF, particularly in regions where NF are highly fragmented (Cheng et al., 2023). We found that the spatial-scale conversion of mixed pixels introduces some uncertainty into the future projections of hydraulic traits, although it does not alter the overall trends of specific trait changes (Figure S7 in Supporting Information S1). Future studies should further improve the spatial and temporal resolution of environmental and ecological factors, as well as retrieved traits, to enhance the predictive accuracy for these mixed pixels. As highlighted by Medlyn et al. (2017) in their study of the hydraulic trait g_1, different methodological approaches each have inherent limitations. Site-level hydraulic traits, while directly and relatively accurately measured at the individual tree level, are typically based on a few days of observation during the growing season and are spatially constrained by limited sampling. In contrast, ecosystem-scale hydraulic traits are derived from inverse modeling approaches aimed at accurately reproducing carbon and water fluxes (Liu, Holtzman, & Konings, 2021). These values are not intended to replicate site-level measurements, but instead reflect ecosystem-scale effective traits, resulting in a scale-gap between ecosystem-scale trait estimates and individual species-level observations (Figure S1 in Supporting Information S1). In addition, the data set used in this study primarily comprises common tree species in China, with a focus on temperate and subtropical broadleaf forests. As such, it may not be representative of tree species in boreal or tropical regions. While the findings may not be directly generalizable to other biomes, the study region—one of the few areas globally that has undergone large-scale, long-term afforestation—provides valuable insights into how afforested species may respond to climate change, thereby advancing our understanding of trait dynamics under afforestation in other regions.

4.3. Future Acclimation of Hydraulic Traits in NF and PF Under Climate Change

Recent studies have confirmed that trait acclimation enhances the potential to predict species vulnerability under climate change scenarios (Liu, Ye, et al., 2022). However, limited research has addressed the computational prediction of plant acclimation to climate change over extended timescales. In this study, we projected future trends of ecosystem-scale hydraulic traits under the assumption of trait acclimation using a

space-for-time substitution approach. However, we acknowledge the uncertainty associated with this assumption, as temporal trait acclimation may diverge from spatial climate–trait relationships due to factors such as species interactions, community turnover, mortality, and lagged responses to climate change. Our approach assumes that the current spatial climate-trait relationship represents the temporal trajectory of trait change. As effects of historical climate change and disturbances prior to 2004 were not considered, the response of hydraulic traits to environmental factors may be overestimated (Kharouba & Williams, 2024). Additionally, we assumed that trait-environment relationships remain constant over time. In reality, as climate conditions deviate from historical norms, trait responses may become nonlinear or even reverse in direction, potentially invalidating the predictions under novel climatic regimes (Kharouba & Williams, 2024). Furthermore, our projections of trait acclimation only incorporated changes in ENV factors, while assuming ECO factors remain static. This exclusion of ecological dynamics under changing climate conditions may limit the accuracy of predicted hydraulic trends. Despite the uncertainties associated with our assumption of perfect acclimation, the projected trait trajectories can be used to quantify the magnitude of functional changes within plant communities. In the future, integrating these projections with trait-based plant hydraulic models holds promise for more systematically disentangling the respective roles of ecological and environmental drivers in shaping the terrestrial carbon cycle (Trugman et al., 2020).

Trait acclimation predictions indicate that the canopy water storage capacity C of NF shows a slight upward trend, whereas the C of PF exhibits a declining trend, although this trend is accompanied by significant uncertainty. Both NF and PF are expected to experience increases in stomatal marginal water-use efficiency g_1 and maximum xylem conductance $g_{p,max}$, which may enhance water-use efficiency and carbon sequestration capacity. Additionally, improvements in embolism resistance in both leaves and xylem ($P50_s$ and $P50_x$) are anticipated, better enabling these forests to cope with drought risks and disturbances brought about by climate change. Overall, while differences in the trait acclimation between NF and PF persist, both systems are expected to evolve toward enhanced water-use efficiency and improved drought resistance in response to rising precipitation and air dryness. As land surface models increasingly integrate explicit representations of plant hydraulics (Anderegg & Venturas, 2020; Lawrence et al., 2019; Li et al., 2021a, 2021b), our study provides a baseline for potential trait shifts under future climatic conditions and offers critical insights into how hydraulic traits of NF and PF may respond to environmental changes through acclimation. This will foster a mechanistic understanding of plant physiological responses to afforestation and contribute to improving predictions of carbon and water fluxes under the dual pressures of climate change and anthropogenic influence.

Conflict of Interest

The authors declare no conflicts of interest relevant to this study.

Data Availability Statement

The ecosystem-scale hydraulic trait data set (C, g_1, $g_{p,max}$, $P50_s$, $P50_x$) was obtained from Liu, Holtzman, and Konings (2021). Environmental drivers (P_r, P_s, R_n, T_a, and T_s) were sourced from the GLDAS data set (Beaudoing et al., 2020; Rodell et al., 2004). Shallow soil moisture (M_s) and vegetation optical depth (VOD) were extracted from AMSRE observations (Parinussa et al., 2016). Leaf area index (LAI) was derived from the MODIS MCD15A3H product (Myneni et al., 2015). Canopy height (H_c) was taken from the global forest height map of Liu, Su, et al. (2022). Forest age (A_t) was sourced from China's annual forest age data set (Cheng et al., 2024). Maximum rooting depth (R_d) was obtained from the global observational synthesis of Fan et al. (2017). All scripts used for data processing, analysis, and figure generation, as well as the site-level hydraulic trait data set are accessible on Zenodo (https://doi.org/10.5281/zenodo.17618780).

Acknowledgments
This research was financially supported by the National Natural Science Foundation of China (Grant 42571045), the National Key R&D Program of China (Grant 2022YFC3003401), the Fundamental and Interdisciplinary Disciplines Breakthrough Plan of the Ministry of Education of China (Grant JYB2025XDXM910), the National Natural Science Foundation of China (Grant 41991231), and the Fundamental Research Funds for the Central Universities (lzujbky-2023-eyt01 and lzujbky-2023-ey09). We acknowledge support from all the scientists and students who participated in field campaigns to investigate site-level hydraulic traits in China. This research was supported by the supercomputing center of Lanzhou University.

References

Allen, R. G., Pereira, L. S., Raes, D., & Smith, M. (1998). Crop evapotranspiration-Guidelines for computing crop water requirements-FAO irrigation and drainage paper 56. *Fao*, *300*(9), D05109. Retrieved from https://www.fao.org/4/X0490E/x0490e00.htm

Anderegg, W. R. (2015). Spatial and temporal variation in plant hydraulic traits and their relevance for climate change impacts on vegetation. *New Phytologist*, *205*(3), 1008–1014. https://doi.org/10.1111/nph.12907

Anderegg, W. R., Konings, A. G., Trugman, A. T., Yu, K., Bowling, D. R., Gabbitas, R., et al. (2018). Hydraulic diversity of forests regulates ecosystem resilience during drought. *Nature*, *561*(7724), 538–541. https://doi.org/10.1038/s41586-018-0539-7

Anderegg, W. R., & Venturas, M. D. (2020). Plant hydraulics play a critical role in Earth system fluxes. *New Phytologist*, *226*(6), 1535–1538. https://doi.org/10.1111/nph.16548

Beaudoing, H., & Rodell, M., & NASA/GSFC/HSL. (2020). GLDAS NOAH land surface model L4 3 hourly 0.25 x 0.25 degree V2.1 [Dataset]. *Greenbelt, Maryland, USA, Goddard Earth Sciences Data and Information Services Center (GES DISC)*. https://doi.org/10.5067/E7TYRXPJKWOQ

Campbell, G. S., & Norman, J. M. (1998). *An introduction to environmental biophysics*. Springer Science & Business Media, Springer.

Cheng, K., Chen, Y., Xiang, T., Yang, H., Liu, W., Ren, Y., et al. (2024). A 2020 forest age map for China with 30 m resolution. *Earth System Science Data*, *16*(2), 803–819. https://doi.org/10.5194/essd-16-803-2024

Cheng, K., Su, Y., Guan, H., Tao, S., Ren, Y., Hu, T., et al. (2023). Mapping China's planted forests using high resolution imagery and massive amounts of crowdsourced samples. *ISPRS Journal of Photogrammetry and Remote Sensing*, *196*, 356–371. https://doi.org/10.1016/j.isprsjprs.2023.01.005

Fan, Y., Miguez-Macho, G., Jobbágy, E. G., Jackson, R. B., & Otero-Casal, C. (2017). Hydrologic regulation of plant rooting depth. *Proceedings of the National Academy of Sciences*, *114*(40), 10572–10577. https://doi.org/10.1073/pnas.1712381114

Grossiord, C., Buckley, T. N., Cernusak, L. A., Novick, K. A., Poulter, B., Siegwolf, R. T., et al. (2020). Plant responses to rising vapor pressure deficit. *New Phytologist*, *226*(6), 1550–1566. https://doi.org/10.1111/nph.16485

Hajek, P., Kurjak, D., von Wühlisch, G., Delzon, S., & Schuldt, B. (2016). Intraspecific variation in wood anatomical, hydraulic, and foliar traits in ten European beech provenances differing in growth yield. *Frontiers of Plant Science*, *7*, 791. https://doi.org/10.3389/fpls.2016.00791

Hua, F., Bruijnzeel, L. A., Meli, P., Martin, P. A., Zhang, J., Nakagawa, S., et al. (2022). The biodiversity and ecosystem service contributions and trade-offs of forest restoration approaches. *Science*, *376*(6595), 839–844. https://doi.org/10.1126/science.abl4649

Huang, H., Han, Y., Cao, M., Song, J., & Xiao, H. (2016). Spatial-temporal variation of aridity index of China during 1960–2013. *Advances in Meteorology*, *2016*(1), 1536135. https://doi.org/10.1155/2016/1536135

Huo, J., Shi, Y., Chen, J., Zhang, H., Feng, L., Zhao, Y., & Zhang, Z. (2022). Hydraulic trade-off and coordination strategies mediatfed by leaf functional traits of desert shrubs. *Frontiers in Plant Science*, *13*, 938758. https://doi.org/10.3389/fpls.2022.938758

Jin, Y., Ye, Q., Liu, X., Liu, H., Gleason, S. M., He, P., et al. (2024). Precipitation, solar radiation, and their interaction modify leaf hydraulic efficiency–safety trade-off across angiosperms at the global scale. *New Phytologist*, *244*(6), 2267–2277. https://doi.org/10.1111/nph.20213

Kamruzzaman, M., Jang, M. W., Cho, J., & Hwang, S. (2019). Future changes in precipitation and drought characteristics over Bangladesh under CMIP5 climatological projections. *Water*, *11*(11), 2219. https://doi.org/10.3390/w11112219

Kharouba, H. M., & Williams, J. L. (2024). Forecasting species' responses to climate change using space-for-time substitution. *Trends in Ecology & Evolution*, *39*(8), 716–725. https://doi.org/10.1016/j.tree.2024.03.009

Lawrence, D. M., Fisher, R. A., Koven, C. D., Oleson, K. W., Swenson, S. C., Bonan, G., et al. (2019). The community land model version 5: Description of new features, benchmarking, and impact of forcing uncertainty. *Journal of Advances in Modeling Earth Systems*, *11*(12), 4245–4287. https://doi.org/10.1029/2018MS001583

Li, H., Lu, X., Wei, Z., Zhu, S., Wei, N., Zhang, S., et al. (2021). New representation of plant hydraulics improves the estimates of transpiration in land surface model. *Forests*, *12*(6), 722. https://doi.org/10.3390/f12060722

Li, L., Yang, Z. L., Matheny, A. M., Zheng, H., Swenson, S. C., Lawrence, D. M., et al. (2021). Representation of plant hydraulics in the Noah-MP land surface model: Model development and multiscale evaluation. *Journal of Advances in Modeling Earth Systems*, *13*(4), 1–27. https://doi.org/10.1029/2020MS002214

Liao, C., Luo, Y., Fang, C., Chen, J., & Li, B. (2012). The effects of plantation practice on soil properties based on the comparison between natural and planted forests: A meta-analysis. *Global Ecology and Biogeography*, *21*(3), 318–327. https://doi.org/10.1111/j.1466-8238.2011.00690.x

Liu, H., Gleason, S. M., Hao, G., Hua, L., He, P., Goldstein, G., & Ye, Q. (2019). Hydraulic traits are coordinated with maximum plant height at the global scale. *Science Advances*, *5*(2), eaav1332. https://doi.org/10.1126/sciadv.aav1332

Liu, H., Ye, Q., Gleason, S. M., He, P., & Yin, D. (2021). Weak tradeoff between xylem hydraulic efficiency and safety: Climatic seasonality matters. *New Phytologist*, *229*(3), 1440–1452. https://doi.org/10.1111/nph.16940

Liu, H., Ye, Q., Simpson, K. J., Cui, E., & Xia, J. (2022). Can evolutionary history predict plant plastic responses to climate change? *New Phytologist*, *235*(3), 1260–1271. https://doi.org/10.1111/nph.18194

Liu, X., Su, Y., Hu, T., Yang, Q., Liu, B., Deng, Y., et al. (2022). Neural network guided interpolation for mapping canopy height of China's forests by integrating GEDI and ICESat-2 data. *Remote Sensing of Environment*, *269*, 112844. https://doi.org/10.1016/j.rse.2021.112844

Liu, Y., Holtzman, N. M., & Konings, A. G. (2021b). Global ecosystem-scale plant hydraulic traits retrieved using model-data fusion. *Hydrology and Earth System Sciences*, *25*(5), 2399–2417. https://doi.org/10.5194/hess-25-2399-2021

Liu, Y., Kumar, M., Katul, G. G., Feng, X., & Konings, A. G. (2020). Plant hydraulics accentuates the effect of atmospheric moisture stress on transpiration. *Nature Climate Change*, *10*(7), 691–695. https://doi.org/10.1038/s41558-020-0781-5

Louman, B., Keenan, R. J., Kleinschmit, D., Atmadja, S., Sitoe, A. A., Nhantumbo, I., et al. (2019). *Sdg 13: Climate Action—Impacts on forests and people. Sustainable development goals: Their impacts on forests and people*. Cambridge University Press.

Lu, Y., Duursma, R. A., Farrior, C. E., Medlyn, B. E., & Feng, X. (2020). Optimal stomatal drought response shaped by competition for water and hydraulic risk can explain plant trait covariation. *New Phytologist*, *225*(3), 1206–1217. https://doi.org/10.1111/nph.16207

Maherali, H., Pockman, W. T., & Jackson, R. B. (2004). Adaptive variation in the vulnerability of woody plants to xylem cavitation. *Ecology*, *85*(8), 2184–2199. https://doi.org/10.1890/02-0538

McDowell, N. G., Brodribb, T. J., & Nardini, A. (2019). Hydraulics in the 21st century. *New Phytologist*, *224*(2), 537–542. https://doi.org/10.1111/nph.16151

Medlyn, B. E., De Kauwe, M. G., Lin, Y. S., Knauer, J., Duursma, R. A., Williams, C. A., et al. (2017). How do leaf and ecosystem measures of water-use efficiency compare? *New Phytologist*, *216*(3), 758–770. https://doi.org/10.1111/nph.14626

Mizuta, R., Yoshimura, H., Ose, T., Hosaka, M., & Yukimoto, S. (2019). MRI MRI-AGCM3-2-S model output prepared for CMIP6 HighResMIP [Dataset]. *Earth System Grid Federation*. https://doi.org/10.22033/ESGF/CMIP6.1625

Mizuta, R., Yoshimura, H., Ose, T., Hosaka, M., & Yukimoto, S. (2019). MRI MRI-AGCM3-2-H model output prepared for CMIP6 HighResMIP [Dataset]. *Earth System Grid Federation*. https://doi.org/10.22033/ESGF/CMIP6.10942

Myneni, R., Knyazikhin, Y., & Park, T. (2015). MCD15A3H MODIS/Terra+ Aqua leaf area Index/FPAR 4-day L4 global 500 m SIN grid V006 [Dataset]. *NASA EOSDIS Land Processes DAAC*. https://doi.org/10.5067/MODIS/MOD15A3H.006

Nicotra, A. B., Atkin, O. K., Bonser, S. P., Davidson, A. M., Finnegan, E. J., Mathesius, U., et al. (2010). Plant phenotypic plasticity in a changing climate. *Trends in Plant Science*, *15*(12), 684–692. https://doi.org/10.1016/j.tplants.2010.09.008

Parinussa, R. M., De Jeu, R. A., Van der Schalie, R., Crow, W. T., Lei, F., & Holmes, T. R. (2016). A quasi-global approach to improve day-time satellite surface soil moisture anomalies through the land surface temperature input. *Climate*, *4*(4), 50. https://doi.org/10.3390/cli4040050

Reich, P. B. (2014). The world-wide "fast-slow" plant economics spectrum: A traits manifesto. *Journal of Ecology*, *102*(2), 275–301. https://doi.org/10.1111/1365-2745.12211

Rodell, M., Houser, P. R., Jambor, U. E. A., Gottschalck, J., Mitchell, K., Meng, C. J., et al. (2004). The global land data assimilation system. *Bulletin of the American Meteorological Society*, *85*(3), 381–394. https://doi.org/10.1175/BAMS-85-3-381

Rosas, T., Mencuccini, M., Barba, J., Cochard, H., Saura-Mas, S., & Martínez-Vilalta, J. (2019). Adjustments and coordination of hydraulic, leaf and stem traits along a water availability gradient. *New Phytologist*, *223*(2), 632–646. https://doi.org/10.1111/nph.15684

Shangguan, F., Zhao, M., Zhang, B., Tang, L., Qian, H., Xie, J., & Wang, Z. (2022). Relationship between hydraulic properties and xylem anatomical structure of subtropical plants. *Journal of Zhejiang A&F University*, *39*(2), 252–261. [In Chinese]. https://doi.org/10.11833/j.issn.2095-0756.20210813

Sperry, J. S. (2003). Evolution of water transport and xylem structure. *International Journal of Plant Sciences*, *164*(S3), S115–S127. https://doi.org/10.1086/368398

Sperry, J. S., & Love, D. M. (2015). What plant hydraulics can tell us about responses to climate-change droughts. *New Phytologist*, *207*(1), 14–27. https://doi.org/10.1111/nph.13354

Strutz, T. (2016). *Data fitting and uncertainty: A practical introduction to weighted least squares and beyond* (2nd ed.). Springer Vieweg.

Trugman, A. T., Anderegg, L. D., Shaw, J. D., & Anderegg, W. R. (2020). Trait velocities reveal that mortality has driven widespread coordinated shifts in forest hydraulic trait composition. *Proceedings of the National Academy of Sciences*, *117*(15), 8532–8538. https://doi.org/10.1073/pnas.1917521117

Wang, H., Harrison, S. P., Li, M., Prentice, I. C., Qiao, S., Wang, R., et al. (2022). The China plant trait database version 2. *Scientific Data*, *9*(1), 769. https://doi.org/10.1038/s41597-022-01884-4

Wang, Y., & Frankenberg, C. (2024). Toward more accurate modeling of canopy radiative transfer and leaf electron transport in land surface modeling. *Journal of Advances in Modeling Earth Systems*, *16*(4), e2023MS003992. https://doi.org/10.1029/2023MS003992

Wang, Y., Sperry, J. S., Venturas, M. D., Trugman, A. T., Love, D. M., & Anderegg, W. R. (2019). The stomatal response to rising CO_2 concentration and drought is predicted by a hydraulic trait-based optimization model. *Tree Physiology*, *39*(8), 1416–1427. https://doi.org/10.1093/treephys/tpz038

Wang, Z., Ding, X., Li, Y., & Xie, J. (2022b). The compensation effect between safety and efficiency in xylem and role in photosynthesis of gymnosperms. *Physiologia Plantarum*, *174*(1), e13617. https://doi.org/10.1111/ppl.13617

Yao, G. Q., Nie, Z. F., Zeng, Y. Y., Waseem, M., Hasan, M. M., Tian, X. Q., et al. (2021). A clear trade-off between leaf hydraulic efficiency and safety in an aridland shrub during regrowth. *Plant, Cell and Environment*, *44*(10), 3347–3357. https://doi.org/10.1111/pce.14156

Ye, L. (2021). *The relationship between efficiency and safety of xylem anatomical structure of typical tree species in Tianmu Mountain*. (Master's thesis). Zhejiang A&F University. [In Chinese].

Yi, R., Xu, X., Zhu, S., Zhang, Y., Zhong, F., Zeng, X., & Xu, C. (2021). Difference in hydraulic resistance between planted forest and naturally regenerated forest and its implications for ecosystem restoration in subtropical karst landscapes. *Journal of Hydrology*, *596*, 126093. https://doi.org/10.1016/j.jhydrol.2021.126093

Yu, Z., Liu, X., Zhang, J., Xu, D., & Cao, S. (2018). Evaluating the net value of ecosystem services to support ecological engineering: Framework and a case study of the Beijing plains afforestation project. *Ecological Engineering*, *112*, 148–152. https://doi.org/10.1016/j.ecoleng.2017.12.017

References From the Supporting Information

Choat, B., Jansen, S., Brodribb, T. J., Cochard, H., Delzon, S., Bhaskar, R., et al. (2012). Global convergence in the vulnerability of forests to drought. *Nature*, *491*(7426), 752–755. https://doi.org/10.1038/nature11688

Olson, D. M., Dinerstein, E., Wikramanayake, E. D., Burgess, N. D., Powell, G. V., Underwood, E. C., et al. (2001). Terrestrial ecoregions of the world: A new map of life on Earth: A new global map of terrestrial ecoregions provides an innovative tool for conserving biodiversity. *BioScience*, *51*(11), 933–938. https://doi.org/10.1641/0006-3568(2001)051[0933:TEOTWA]2.0.CO;2